Mechanism of the (^{6}Li, ^{6}He) reaction at intermediate energies and its suitability as a spin probe

J. S. Winfield, N. Anantaraman, Sam M. Austin, Ziping Chen, A. Galonsky, J. van der Plicht,* and H.-L. Wu†
National Superconducting Cyclotron Laboratory and Department of Physics and Astronomy, Michigan State University, East Lansing, Michigan 48824

C. C. Chang
Physics Department, University of Maryland, College Park, Maryland 20742

G. Ciangaru‡
Physics Department, Boston University, Boston, Massachusetts 02215
(Received 23 December 1986)

Angular distributions have been measured for the (^{6}Li, ^{6}He) reaction on targets of ^{7}Li, ^{12,14}C, ^{26}Mg, and ^{90}Zr at bombarding energies of 35, 25, and 14 MeV/nucleon. The ratios of observed cross sections for states in ^{14}N and ^{7}Be suggest that the reaction mechanism is predominantly one-step at 35 and 25 MeV/nucleon with an increasing contribution from sequential transfer at lower energies. Measured forward-angle cross sections for Gamow-Teller transitions are found to be accurately proportional to the corresponding B(GT) values from β^- decay or from (p,n) data. This calibration will allow the measurement of spin-transfer strength with the (^{6}Li, ^{6}He) reaction at intermediate energies. One-step distorted-wave Born approximation calculations, which used Yukawa central and $r^2\times$ Yukawa tensor potentials, are consistent with the data at 35 and 25 MeV/nucleon except for $\theta_{\text{c.m.}}<3°$, and give a central force strength, $V_{\sigma\tau}$, in reasonable agreement with that obtained in (p,n) studies at similar energies per nucleon.

I. INTRODUCTION

For several years the (p,n) reaction with proton energies above 100 MeV has been used successfully in the study of Gamow-Teller (GT) strength in nuclei.[1,2] The quenching of this strength is of great current interest,[3] with implications both for the detailed nuclear structure of the target and for the possible effects of nucleonic excitations. Although most charge-exchange studies have used the (p,n) reaction and, more recently, the (^{3}He,t) reaction,[4] the (^{6}Li,^{6}He) reaction is an alternative choice with several advantages. On the experimental side, the presence of a charged particle in the outgoing channel allows detection by magnetic spectrographs and thus gives potentially better resolution and lower background compared to the (p,n) case. On the theoretical side, the reaction is strongly selective of spin-flip transitions (this is also true of the other reactions, but only at high energies, where $V_{\sigma\tau}$ dominates over V_τ). The suppression of non-spin-flip ($S=0$) transitions and the potentially lower background with the (^{6}Li,^{6}He) reaction may help to locate the "missing" low-lying GT strength.

Some other applications of charge-exchange reactions require excellent energy resolution. An example is the measurement of GT strengths in order to place limits on double-β decay,[5] for which a number of 1^+ states have to be picked out from nearby states of other J^π. Similarly, knowledge of GT strength is needed to calibrate nucleocosmochronometers through β^--decay systematics for low-lying states near the Pb region.[6] A recent application of the (p,n) reaction has been in the search for pion precursor phenomena[7] through isovector 0^+ to 0^- transitions, for which the spin-flip component of the nuclear interaction is expected[8] to couple strongly with the pion propagator in nuclear matter and give enhanced cross sections for momentum transfers of about two to three times the pion mass. Suitable 0^- states in ^{16}F and ^{14}N are only weakly populated and are separated by $\approx$200 keV from neighboring states.

Another aspect of charge exchange with heavy ions such as ^{6}Li is the strong attenuation of the projectile wave function inside the target nucleus, which means that the reactions selectively sample the nuclear surface, unlike the nucleon-induced case.

If the (^{6}Li,^{6}He) reaction is to be used as a spin-transfer probe,[9,10] it is important that the reaction mechanism be shown to be one-step, because then the following selection rules apply:

$$\pi=(-)^L ,$$

$$\pi'=(-)^{L'} ,$$

$$S=S' ,$$

where π, L, and S denote the parity, orbital angular momentum, and spin transfer in the projectile system, and π', L', and S' are the same quantities in the target system (there is a weak violation of these rules in the presence of nonlocal exchange terms). For ^{6}Li(1^+)$\rightarrow$^{6}He(0^+), the

parity selection rule requires L to be even and the angular momentum coupling allows only spin transfers of $S=1$. The parity rules do not hold for sequential transfer processes, involving, e.g., $^6\text{Li}\rightarrow{}^7\text{Li}\rightarrow{}^6\text{He}$,[11] although they may be partially recovered if the reaction is localized such that the pickup and stripping occur close to the same point. At the low bombarding energies (32–62 MeV) at which most previous experiments have been performed, there has been much debate[12–17] over the relative importance of the single-step and sequential transfer processes. However, the second-order processes are expected[18,19] to become less important as the bombarding energy is increased, as a consequence of the decreasing overlap of the projectile and target momentum distributions. Indeed, it has recently been claimed[20] that one-step calculations are consistent with data for $^{14}\text{C}(^6\text{Li},^6\text{He})^{14}\text{N}$ at 93 MeV. As another reference point, the (p,n) reaction appears[21] to be well described by the one-step mechanism at energies above 25 MeV.

Assuming that the one-step mechanism is dominant, GT strength may be measured at forward angles and high bombarding energies where $L'=0$ transfers are strong. At more backward angles (or lower bombarding energies), higher multipolarity spin-flip excitations may be observed. A critical issue, if the (^{6}Li,^{6}He) reaction is to be used as a probe for spin transfer strength, is whether the measured GT cross sections are proportional to the squares of the corresponding β-decay matrix elements, as has been found[2] in (p,n) reactions above 100 MeV. For the (^{6}Li,^{6}He) reaction at 5 MeV/nucleon, Wharton and Debevec[13] found a smooth but pronounced mass dependence in the ratio of cross sections to GT strength. Such a mass dependence is obviously undesirable if the (^{6}Li,^{6}He) reaction is to be used to extend the range of measured GT matrix elements, but we show here that it is ameliorated at higher bombarding energies.

In this paper we present a systematic survey of GT transitions induced by the (^{6}Li,^{6}He) reaction at $E/A=14$, 25, and 35 MeV on a wide range of target nuclei ($A=7$–90). Some of the data at 35 MeV/nucleon have been reported in a previous Letter.[22] We describe two kinds of tests of the reaction mechanism. The simpler one (Sec. III A) involves the comparison of cross section ratios for final states in ^{14}N and ^{7}Be. The second is the comparison of the experimental cross sections with one-step distorted-wave Born approximation (DWBA) predictions (Sec. IV). The calculations yield estimates of the central and tensor force strengths. Next, in Sec. V, we investigate the correlation between the measured (^{6}Li,^{6}He) cross sections at forward angles and the corresponding GT strengths. We summarize our results and present our conclusions in Sec. VI.

II. EXPERIMENTAL PROCEDURES

The experiment was performed with beams of 14, 25, and 35 MeV/nucleon (83.4, 150, and 210 MeV) ^{6}Li ions from the K500 cyclotron at the National Superconducting Cyclotron Laboratory. Typical beam currents on target were about 30 particle nA. The targets bombarded were ^{7}Li and ^{12,14}C (all energies), ^{26}Mg (35 MeV/nucleon only), and ^{90}Zr (25 and 35 MeV/nucleon). Self-supporting ^{7}Li targets of thicknesses 4.9 and 4.5 mg/cm^2 were manufactured by rolling oil-immersed pieces of the metal; the targets were then transferred to the target chamber under vacuum. The 440 μg/cm^2 ^{14}C target was obtained from Chalk River Nuclear Laboratory. The thicknesses of the other targets were 475 μg/cm^2 (^{12}C), 1.08 mg/cm^2 (^{26}Mg), and 2.08 mg/cm^2 (^{90}Zr). All the target thicknesses were measured by the α-particle energy-loss technique after the experiment was completed.

The ^{6}He reaction products were momentum-analyzed by the S-320 spectrograph[23] which can bend ^{6}He ions up to 35.6 MeV/nucleon. A typical solid angle was 0.25 msr with $\pm 0.3°$ horizontal angular acceptance. The focal plane detector consisted of two position sensitive proportional counters, an ion chamber for energy-loss information, and a stopping plastic scintillator which provided both a measure of the total energy of the particles and a stop signal for time-of-flight (TOF) relative to the cyclotron frequency (rf). The ^{6}He particle group was cleanly identified in plots of energy-loss versus scintillator light output (Fig. 1). The TOF signal was used as an additional gate to exclude any background events with anomalous total-energy signals. The spectra shown in the following section have little remaining background—a fact that may be attributed in part to the high magnetic rigidity of the $^6\text{He}^{2+}$ ions. Typically, a resolution of $\Delta E/E=1/600$ was obtained. Although this is quite modest compared to a state-of-the-art heavy-ion spectrograph, the absolute resolution at the lowest bombarding energy was significantly better than that obtained in intermediate-energy (p,n) experiments.

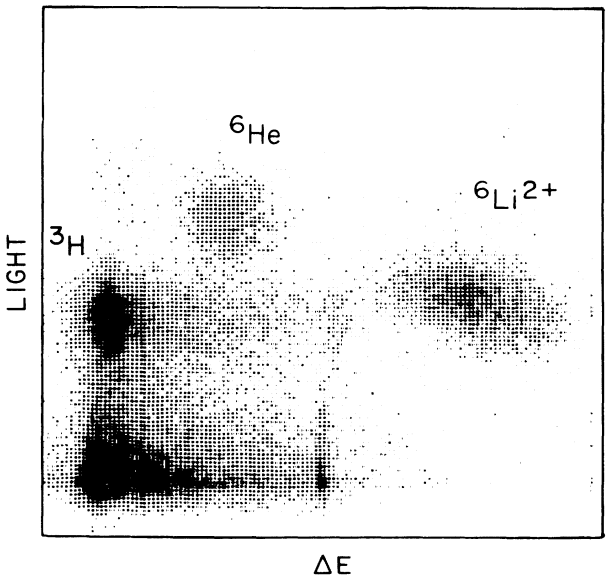

FIG. 1. Particle identification plot for 35 MeV/nucleon ^{6}Li on ^{12}C with the spectrograph positioned at 0° and the field set to detect ^{6}He reaction products. LIGHT is the output from the stopping scintillator at the back of the focal plane detector, ΔE is the ion-chamber (energy-loss) signal.

The relative normalizations between the different angular settings of the spectrograph were based on the integrated current from a Faraday cup located about 1.5 m from the target. This Faraday cup was in the form of a long horizontal plate which moved with the rotation of the spectrograph. The charge collection efficiency for different angle settings was calibrated by comparing measured cross sections of elastic scattering from a gold target to optical model predictions in the Coulomb-dominated region. In addition, elastic scattering peaks were recorded in three monitor detectors (3 mm thick plastic scintillators) set at fixed angles to the beam. Corrections to the measured integrated current from the Faraday cup were required only for the smallest angles ($\theta_{\text{lab}} < 3°$) where edge effects of the plate would be expected to be important.

As a check of the cross section normalization, some limited elastic scattering angular distributions were measured at the 35 MeV/nucleon bombarding energy. By comparing these data with cross section calculations which used optical model (OM) potentials from the compilation of Cook *et al.*,[24] we estimate the overall normalization uncertainty arising mainly from the beam integration and the target thickness measurement to be about $\pm 10\%$. This is not included in the errors shown in the angular distributions. Owing to the small angular range covered and the uncertainty in the true scattering angle (estimated at $\pm 0.1°$), it was not feasible to obtain new optical model potentials from the data. However, one may obtain some indication of the applicability of the potentials from Cook *et al.* from the shape of the angular distributions. Although these potentials were determined from 156 MeV ^{6}Li scattering data, they give a good reproduction of the present ^{6}Li + ^{12}C, ^{6}Li + ^{26}Mg, and ^{6}Li + ^{90}Zr data at 210 MeV (Fig. 2), although some inadequacies are apparent for ^{6}Li + ^{14}C. This may be of relevance to the DWBA calculations for the reaction (Sec. IV) which used the same optical parameters.

Measurements of the ^{12}C(^{6}Li,^{6}He)^{12}N and ^{14}C(^{6}Li,^{6}He)^{14}N reactions with the spectrograph positioned at 0° were undertaken at 35 MeV/nucleon. At this position the finite solid angle of acceptance lead to a mean laboratory angle of 0.3°. With the spectrograph set to bend ^{6}He^{2+} ions to the focal plane, the ^{6}Li^{3+} ions, which are the major charge state component at this energy, were bent away from the detector, but the ^{6}Li^{2+} ions would still have been intense enough to cause a count-rate problem if allowed to enter the focal plane detector. (From other parts of the experiment the ^{6}Li^{2+}/^{6}Li^{3+} ratio at 35 MeV/nucleon was measured to be about 7×10^{-6} with the Zr target and about 1.2×10^{-6} with the Mg target.) Accordingly, a blocking finger immediately upstream of the detector was positioned to catch the ^{6}Li^{2+} ions; the negative Q value of the (^{6}Li,^{6}He) reaction results in the ^{6}He^{2+} ions being shifted by a few centimeters along the focal plane away from the finger. Since no Faraday cup was in place for these measurements, the cross sections were deduced from the counts in the monitor detectors.

The focal plane of the spectrograph was calibrated by varying the magnetic elements to step the elastic scattering group across the region of interest. The calibration points were fitted by a second-order polynomial.

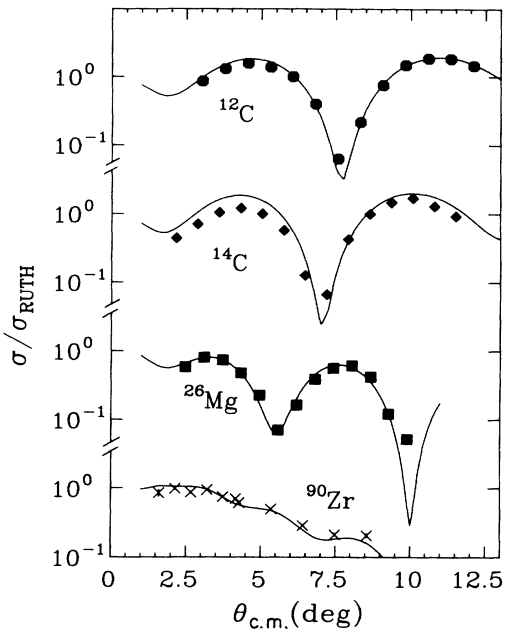

FIG. 2. Angular distributions for the elastic scattering of 35 MeV/nucleon ^{6}Li from ^{12}C, ^{14}C, ^{26}Mg, and ^{90}Zr. An angle uncertainty of $\pm 0.1°$ is not included in the error bars. The curves are optical model calculations as described in the text.

III. ANALYSIS

A. Discussion of the spectra and ratio tests of the reaction mechanism

Two of the targets studied here, ^{14}C and ^{7}Li, provide final states which may be used in simple tests of the reaction mechanism. For ^{14}N, we compare the yield to the 3.95 MeV 1^+ state, which should be strongly populated by the one-step process (due to a large GT matrix element), with the yield to two states that are inhibited in the one-step process (either because of a small GT matrix element or because spin transfer $S=1$ is forbidden). For the ^{7}Li target, we compare forward angle yields for two transitions, $\frac{3}{2}^-$ to $\frac{3}{2}^-$ and $\frac{3}{2}^-$ to $\frac{1}{2}^-$. For $L'=0$ transfer, the second of these is purely $S=1$ (GT), while the first may have also an $S=0$ (Fermi) component unless the (^{6}Li,^{6}He) reaction is one-step.

The ratio tests ought to be insensitive to the details of the reaction mechanism since any kinematic effects should nearly cancel in the ratio and one does not need to know details of the nuclear structure involved. In practice, however, exchange and tensor amplitudes in the one-step process will always be present to some extent and one may well not obtain precisely the ratios of strengths observed in β decay, even if sequential transfer processes in the reaction are negligible. An additional complication is that not only the single-step but also the sequential-transfer process tends to populate states in proportion to the corresponding β-decay matrix elements.[13,25]

1. $^{14}C(^6Li,^6He)^{14}N$

Spectra for the reaction on the ^{14}C target at the three bombarding energies are presented in Fig. 3. The ^{14}C target was studied in more detail than the others, mainly because of three levels in ^{14}N that provide a useful test of the reaction mechanism. The 1^+ ground state has a B(GT) value from β decay only about 10^{-6} (Ref. 26) of that for the strong 3.95 MeV 1^+ level (which contains more than 90% of the low-lying GT strength[14,15] in ^{14}N). The ratios of (^{6}Li,^{6}He) cross sections to these states (all taken at $q \approx 100$ MeV/c) are shown by the upper set of points in Fig. 4 as a function of bombarding energy; the point at $E/A = 10$ MeV has been extracted from Ref. 15. For comparison, in the (p,n) reaction at 35 MeV,[27] the ratio of yields was found to be 0.17, while at 160 MeV,[28] it had dropped to 0.01. However, tensor and $L=2$ central amplitudes may account at least in part for the observed energy dependence of the ratios and the apparent discrepancy with the β-decay ratio. A better test of the contribution of two-step processes is the ratio of the 0^+ isobaric analog state (IAS) at 2.31 MeV to the 3.95 MeV state, because a 0^+ to 0^+ transition can only be mediated by the nonlocal part of the exchange interaction in a one-step mechanism. It is known[29] that this is an $L=1$ process which would be weak near 0°. The ratio, plotted as the lower set of points in Fig. 4, shows that the IAS is suppressed by a factor of 2 at $E/A=35$ and 25 MeV compared with the lower bombarding energies, which suggests that multistep processes are less significant at the higher energies. We note that the intrinsic strength of the IAS transition would be about the same as that of the 3.95 MeV state if $S=0$ transfer were not forbidden, since the GT matrix element is about 1.5 times larger than the Fermi matrix element but is compensated by $V_\tau \approx 1.4 V_{\sigma\tau}$ at this energy per nucleon.[21] For the ^{14}C(p,n)^{14}N reaction at 35 MeV,[27] the ratio σ(IAS)/σ(3.95) is 0.8, which illustrates the lack of $S=1$ selectivity in low energy (p,n) reactions. The value of 0.05 observed with the (^{6}Li,^{6}He) reaction at 35 MeV/nucleon thus corresponds to a suppression of $S=0$ strength by a factor of 16.

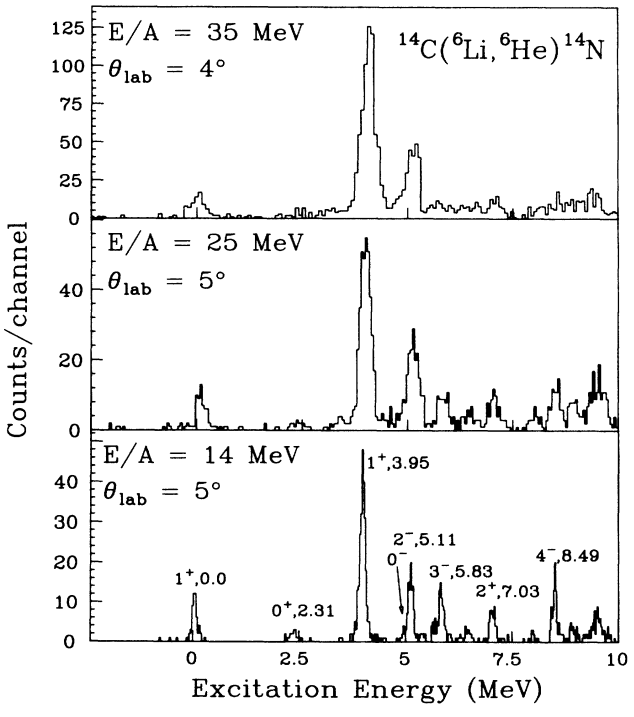

FIG. 3. Spectra for ^{14}C(^{6}Li,^{6}He)^{14}N for E(^{6}Li)=14, 25, and 35 MeV/nucleon. States in ^{14}N are indicated, with the excitation energy given in MeV. The energy resolution is about 1 in 600.

2. $^7Li(^6Li,^6He)^7Be$

The resolution observed in the ^{6}He spectra for the ^{7}Li target (Fig. 5) is dominated by target thickness at 14 MeV/nucleon and by the worsening absolute energy resolution of the spectrograph at 35 MeV/nucleon. Only at 25 MeV/nucleon are the ground state and 0.43 MeV first excited state of ^{7}Be resolved, but, with the reasonable assumption of equal FWHM, yields to these two states could be determined from a peak-fitting program with sufficient accuracy at all energies.

A test of whether one-step processes are dominant, similar to the tests described above for the ^{14}C target, is to compare the ratio of forward-angle (thus, ideally, $L'=0$) cross sections for the $\frac{3}{2}^-$ ground and $\frac{1}{2}^-$ 0.43-MeV states of ^{7}Be with the ratio, 1.18, of B(GT) values known from β decay. If the reaction is purely one-step, the $S=0$ (Fermi) transfer in the $\frac{3}{2}^-$ to $\frac{3}{2}^-$ transition will be forbidden. The ratios of yields from the (^{6}Li,^{6}He) reaction (Table I) for a given energy are seen to depend on angle, with the smallest angle studied generally giving a lower value in each case. This is possibly due to the effects of tensor and $L=2$ central amplitudes at larger angles [note the angle dependence of the tensor interaction effects in the ^{7}Li(p,n)^{7}Be reaction analysis of Austin *et al.*[30]]. In any case, only at $E/A=35$ MeV is the (^{6}Li,^{6}He) ratio (at $\theta=2.5°$) in agreement with the B(GT) ratio. There is a trend away from this value as the bombarding energy is reduced, which suggests that the reaction mechanism is

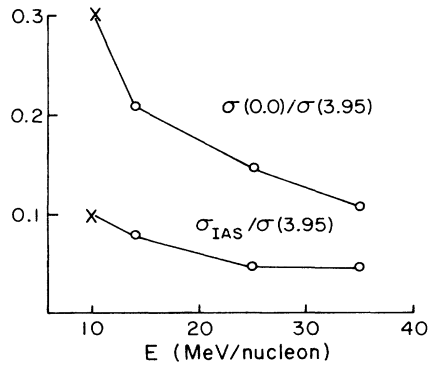

FIG. 4. Plot of the ratios of cross sections at $q \approx 100$ MeV/c for $^{14}N_{g.s.}$ and $^{14}N_{IAS}$ to $^{14}N_{3.95}$ vs bombarding energy. The values for the 10 MeV/nucleon points are taken from Ref. 15.

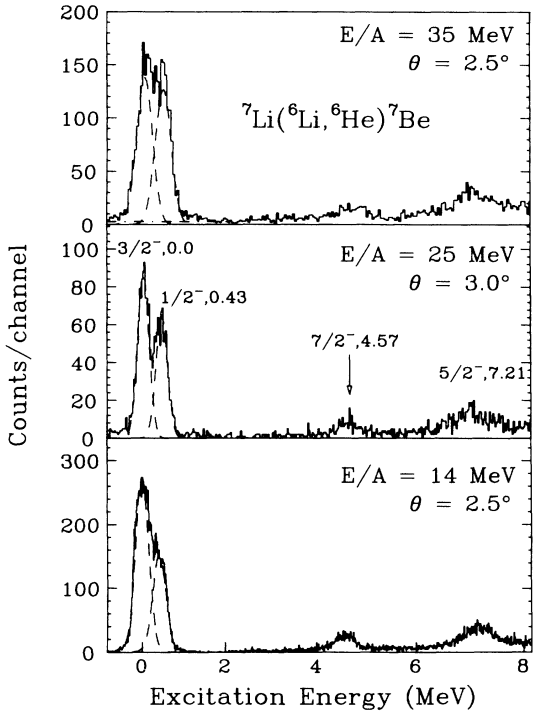

FIG. 5. Spectra for ^{7}Li(^{6}Li,^{6}He)^{7}Be at 14, 25, and 35 MeV/nucleon. The dashed lines show the fits to the ground and 0.43 MeV excited states of ^{7}Be.

predominantly one-step at 35 MeV/nucleon with sequential transfer processes becoming more important at lower energies.

3. $^{12}C(^{6}Li,^{6}He)^{12}N$ and $^{26}Mg(^{6}Li,^{6}He)^{26}Al$

Spectra for the ^{12}C and ^{26}Mg targets are shown in Fig. 6. The GT states of interest are the ground state of ^{12}N, the 1.06 MeV state of ^{26}Al, and two levels at 1.85 and 2.07 MeV of ^{26}Al which were unresolved. The GT matrix elements for these states are known from β decay (see the compilation in Ref. 2) and are compared with our measured cross sections in Sec. V.

TABLE I. Ratios of yields to ^{7}Be$_0$ and ^{7}Be$_1$ for different ^{6}Li bombarding energies. The second column shows the unweighted mean of the ratios for all angles studied (typically from 2.5° to 5.5° lab); the uncertainty given is the standard deviation of the measured results about the mean. The third column gives the ratio at the smallest angle only (the uncertainty is the statistical error from the fit). The ratio expected from β decay is 1.18.

E/A	$\sigma(\frac{3}{2}^-,0.0)/\sigma(\frac{1}{2}^-,0.43)$	
(MeV)	all θ's	$\theta \approx 2.5°$
35	1.46±0.10	1.08±0.06
25	1.47±0.08	1.34±0.07
14	1.66±0.06	1.78±0.05

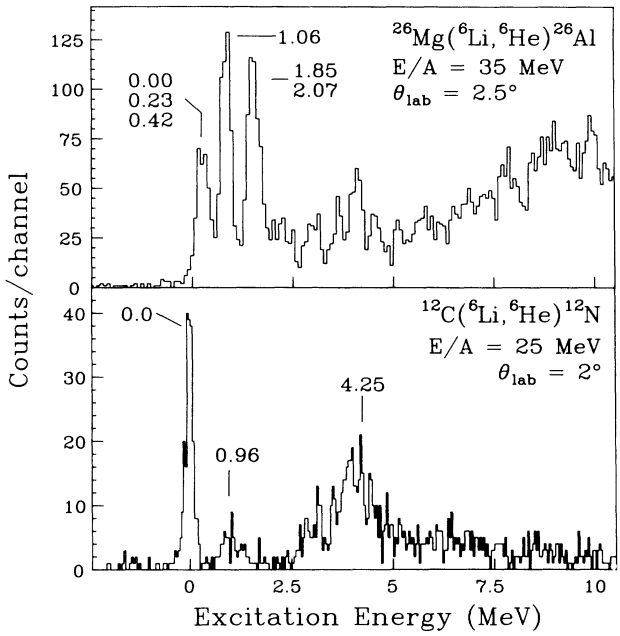

FIG. 6. Spectra for ^{12}C(^{6}Li,^{6}He)^{12}N for $E(^{6}\text{Li})=25$ MeV/nucleon and ^{26}Mg(^{6}Li,^{6}He)^{26}Al for $E(^{6}\text{Li})=35$ MeV/nucleon.

4. $^{90}Zr(^{6}Li,^{6}He)^{90}Nb$

A spectrum for the reaction on the ^{90}Zr target at 35 MeV/nucleon is shown in Fig. 7. The spectrum is clean in the sense that little background is observed in the channels below the ground state of ^{90}Nb. The peak at 2.3 MeV excitation in ^{90}Nb is taken to correspond to the peak at the same excitation seen in the (p,n) reaction at 120 MeV,[31] where it was identified as a cluster of 1^+ levels. The peak at 1.0 MeV also was observed in the (p,n) study

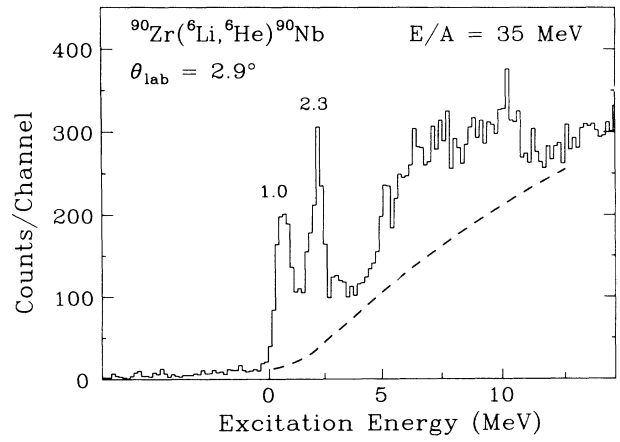

FIG. 7. Spectrum for ^{90}Zr(^{6}Li,^{6}He)^{90}Nb at 35 MeV/nucleon and a laboratory angle of 2.9°. The dashed line is a background drawn by hand to represent the $\Delta L \geq 1$ contribution.

and was deduced to have contributions mainly from multipoles higher than $L=0$.

Above the two sharp peaks, one observes a broad feature in the (^{6}Li,^{6}He) spectrum which is centered at approximately 8.5 MeV excitation in ^{90}Nb. This corresponds to the giant GT resonance (GTR) as observed in the (p,n) study,[31] for which the excitation energy was estimated as 8.7 ± 0.3 MeV. The structure at 8.5 MeV in Fig. 7 has a linear momentum transfer (q) similar to that for ^{90}Zr(p,n)^{90}Nb at $E_p=120$ MeV and 11.5°, and indeed the present ^{90}Zr(^{6}Li,^{6}He) spectrum shows an overall resemblance to the 10° (p,n) spectrum of Bainum *et al.*,[31] except that the IAS is not clearly seen. Alternatively, one can compare with the discovery spectrum[32] for the GTR taken at $E_p=45$ MeV, which is again similar to that shown in Fig. 7.

Closer inspection of the GTR region in Fig. 7 suggests that it may be composed of two broad peaks at approximately 7 and 10 MeV excitation. In a study of ^{90}Zr(^{6}Li,^{6}He)^{90}Nb at 15.5 MeV/nucleon, Dem'yanova *et al.*[33] also observed an apparently double-peaked broad structure at similar excitation in the most forward angle spectra. They have calculated the contributions from different L for $q\approx1.2$ fm^{-1} ($\theta_{c.m.}=13°$ in their case): the $L=0$ strength is about 15% of that from $L=1$ and $L>1$ combined, and these higher multipole transitions account for the double-peaked appearance of the spectrum near the GTR. In our case ($q\approx0.5$ fm^{-1}) we would expect relatively more contribution from $L=0$. If a simple smooth background is drawn to represent the underlying $L\geq1$ strength, the ratio of the broad peak to the 2.3-MeV peak is 4.0, which agrees with the ratio, 4.6 ± 0.7, of B(GT) values found in the (p,n) work.[31] Alternatively, one can use the ratio of yields of the 2.3-MeV peak and the GTR from the (p,n) spectrum to estimate that about 40% of the (^{6}Li,^{6}He) cross section between 6 and 11 MeV is from the GTR.

B. Shapes of angular distributions

One expects that the shapes of the various GT angular distributions, when plotted as cross sections vs qR, where R is the sum of the target and projectile radii, should be the same if the same reaction mechanism is acting and if distortion effects are similar for different transitions. Figure 8 shows that this is roughly true. It is interesting however, that the position of the second maximum in the angular distribution for ^{14}C(^{6}Li,^{6}He)^{14}N (3.95 MeV) appears to move from about 120 MeV/c at $E(^6\text{Li})=14$ MeV/nucleon to about 100 MeV/c at $E(^6\text{Li})=35$ MeV/nucleon. The 15.5 MeV/nucleon data of Aleksandrov *et al.*[20] and the 10 MeV/nucleon data of Wharton *et al.*[15] peak at about 120 MeV/c. The shift at the higher energy and less pronounced peak in the 25 MeV/nucleon data may be due to the different contributions from the tensor force to the cross section at these energies.

In Fig. 9 the angular distributions for the 1^+ ground and 0^+ 2.31-MeV states in ^{14}N are compared with that for the GT 3.95-MeV state. The shapes of the distributions for the two 1^+ states are markedly similar, whereas the IAS state is clearly distinct.

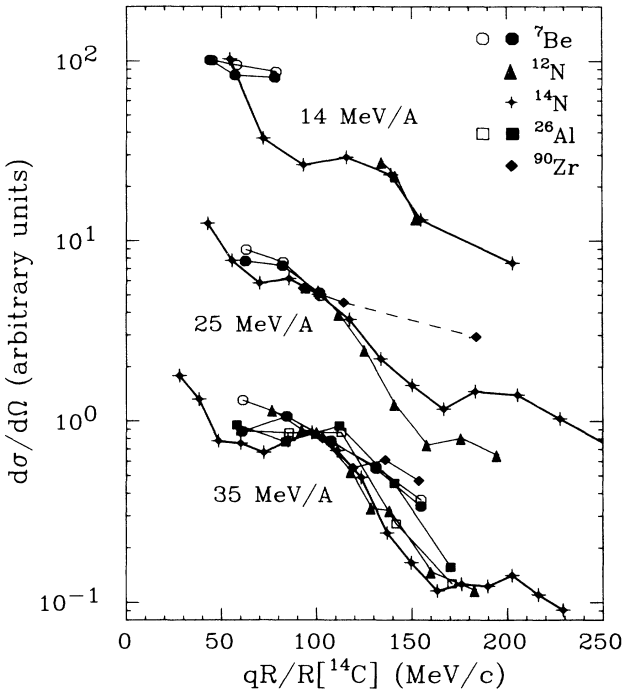

FIG. 8. Angular distributions for various GT transitions plotted vs $qR/R(^{14}\text{C})$, where $R/R(^{14}\text{C})$ is the sum of the projectile and target radii divided by that of ^{6}Li+^{14}C. The lines connect the data points and are to guide the eye. At each energy, the distributions for a given target and final state are normalized by eye to that for ^{14}C (thick line). For ^{7}Be (^{26}Al), the filled symbol corresponds to the 0.0 MeV (1.06 MeV) state and the open symbol corresponds to the 0.43 MeV (1.85 MeV) state.

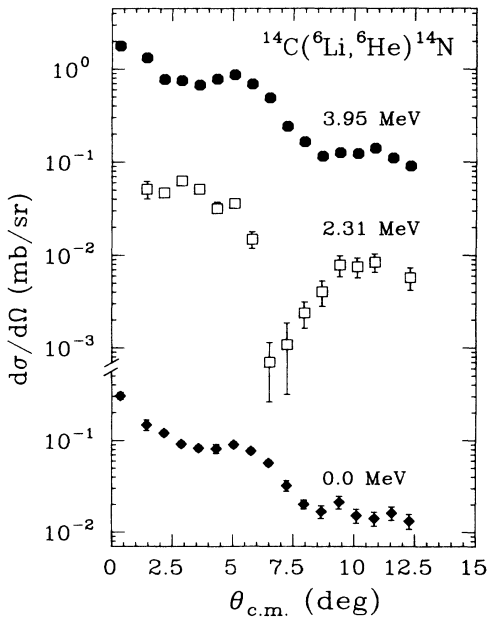

FIG. 9. Experimental angular distributions for the 1^+ (0.0 MeV), 0^+ (2.31 MeV), and 1^+ (3.95 MeV) states in ^{14}N from the reaction ^{14}C(^{6}Li,^{6}He)^{14}N at $E(^6\text{Li})=35$ MeV/nucleon.

IV. ONE-STEP DWBA PREDICTIONS

A second class of reaction mechanism tests is the comparison of data with one-step distorted-wave Born approximation (DWBA) calculations. The DWBA code used is a modified version[17] of DWUCK4 (Ref. 34) which allows for the finite size and cluster structure of the projectile system and includes direct central ($V_{\sigma\tau}$) and tensor terms in the interaction. Knockon exchange corrections corresponding to the central interaction are included through the local-energy approximation method; for further details, see Ref. 17.

The direct (central) interaction had a Yukawa form with a 1 fm range. This value for the range is commonly used in (p,n) analyses at low energies, but it might be considered somewhat small for heavy-ion-induced reactions in view of the strong absorption of the composite projectile.[35] As a check, a test calculation with a 1.4 fm range was performed for ^{14}C(^{6}Li,^{6}He)^{14}N and compared to a calculation with the 1.0 fm range [for convenience, the modified[36] code SATURN-MARS (Ref. 37) was used for these tests]. The cross section predicted with the 1.4 fm range force was 33% larger than that for a 1.0 fm range force with the same volume integral. The effect is thus fairly small in comparison with other uncertainties; it would decrease the $V_{\sigma\tau}$ extracted from a cross section fit by about 15%.

As in Ref. 17, the form of the tensor interaction was an $r^2\times$Yukawa with a range of 1.0 fm. In the DWBA calculations described below, it will be seen that the tensor force introduces a significant $L=2$ component to the cross section. Due to the noncentral character of the two-body tensor interaction, orbital angular momenta differering by two units may be transferred to the projectile (L) and to the target (L'). For 0^+ to 1^+ transitions, the allowed combinations of L and L' are

$$L=0,\quad L'=2$$

and

$$L=2,\quad L'=0,2\ .$$

The strong absorption characteristic of heavy-ion reactions favors the larger L transfer,[38] which accounts for the observed $L=2$ strength. The tensor force tends to favor $L\neq L'$,[38] in contrast to the central force, for which $L=L'$ always. Thus, despite the significant $L=2$ tensor component to the cross section, the transitions are expected to be predominantly Gamow-Teller ($L'=0$) in the target system.

A. ^{14}N (3.95 MeV)

Angular distributions are shown in Fig. 10 for the ^{14}N 1^+, 3.95-MeV final state at the three energies studied. For the 35 and 25 MeV/nucleon calculations, an optical potential obtained[24] from 156 MeV ^{6}Li elastic scattering on ^{12}C was used in both the entrance and exit channels; the potential is listed as $C1$ in Table II. A global ^{6}Li potential from Ref. 39 was used in the 14 MeV/nucleon calculation ($C2$ in Table II). Wave functions for the target system were obtained from $1p$ shell-model calculations with an interaction of Millener.[40] They were renormalized to give the experimental B(GT) value as indicated in Table III. This renormalization effectively increased the extracted $V_{\sigma\tau}$ strength by approximately 20%.

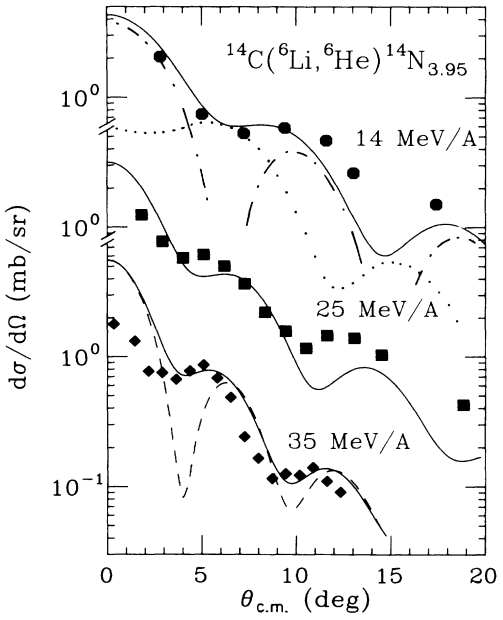

FIG. 10. Angular distributions for the reaction ^{14}C(^{6}Li,^{6}He)^{14}N (1^+, 3.95 MeV) at $E(^{6}\text{Li})=14$, 25, and 35 MeV/nucleon. The solid curves are microscopic DWBA predictions, with central (direct plus exchange) and tensor terms included ($V_{\text{ten}}/V_{\sigma\tau}=0.135$). The dashed line is a calculation for $E=35$ MeV/nucleon with only the central (direct plus exchange) terms. The dash-dotted and dotted lines are the calculated $L=0$ and $L=2$ components, respectively, of the cross section for $E=14$ MeV/nucleon. The calculations are normalized to the data (excluding $\theta_{\text{c.m.}}<3°$ for $E_{\text{Li}}=35$ MeV/nucleon) to yield the empirical strengths of the interaction shown in Table IV.

The 35 MeV/nucleon calculations overpredict the data at small angles (it appears that the overprediction is not as bad for 25 and 14 MeV/nucleon), and in the following we discuss two possible reasons. First, the choice of OM potentials might be questioned, especially in view of the poor reproduction of our ^{6}Li+^{14}C elastic scattering data (Sec. II). A preliminary potential from McMaster *et al.*[41] ($M1$ in Table II), which was obtained from a fit to 35 MeV/nucleon ^{6}Li+^{12}C data, was also tried in a ^{14}C(^{6}Li,^{6}He)^{14}N calculation. This yielded results similar to those with the Cook *et al.*[24] potential, both in terms of the shape of the angular distribution and the overall magnitude. We cannot preclude the possibility that some other potential might give a better fit at small angles, but it seems unlikely. A more probable reason for the overprediction at small angles is the neglect of the exchange part of the tensor interaction. Inclusion of this term would involve a formidable calculation for heavy ions,[42] but comparison with exact (p,n) calculations suggests that the effect would be to lower the calculated cross section in the forward angle region.

TABLE II. Optical model parameters deduced from ^{6}Li elastic scattering and used in the present (^{6}Li,^{6}He) DWBA calculations. Both real and imaginary potentials are of the volume Woods-Saxon form. The convention $R_x = r_x A_T^{1/3}$ is followed.

	V (MeV)	a_v (fm)	r_v (fm)	W (MeV)	a_w (fm)	r_w (fm)	Ref.
$C1$[a]	112.1	0.816	1.3	32.1	0.808	1.7	24
$C2$[b]	109.5	0.811	1.326	c	0.884	1.534	39
$M1$[d]	121.7	0.818	1.206	37.72	0.865	1.546	41

[a]Used for ^{12,14}C(^{6}Li,^{6}He) at 35 MeV/nucleon and ^{14}C(^{6}Li,^{6}He) at 25 MeV/nucleon.
[b]Used for ^{14}C(^{6}Li,^{6}He) at 14 MeV/nucleon and ^{26}Mg(^{6}Li,^{6}He) at 35 MeV/nucleon.
[c]$W = 58.16 - 0.328A + 0.00075A^2$.
[d]Alternative potential used for ^{14}C(^{6}Li,^{6}He) at 35 MeV/nucleon.

For the 35 MeV/nucleon case, we normalized the DWBA cross sections to the data for $\theta_{c.m.} > 3°$. If all the data were included, the fitted cross section would be about 50% lower, which would give a 30% smaller value of $V_{\sigma\tau}$. The values for the three energies studied here are listed in Table IV; also indicated are the values of $V_{\sigma\tau}$ required to fit the data at 35 MeV/nucleon with the tensor or exchange part of the central interaction omitted. The values of $V_{\sigma\tau}$ from the present analyses may be compared with the average value of 11.7 ± 1.7 MeV obtained[43] from (p,n) and (p,p') studies at similar energies per nucleon. While the strengths obtained for the 35 and 25 MeV/nucleon data are in good agreement with this value, the 14 MeV/nucleon value shows a marked discrepancy. We note, however, that the latter calculation was done with an optical potential different from the others. As a check of the 14 MeV/nucleon result, we may compare with Aleksandrov *et al.*[20] who studied ^{14}C(^{6}Li,^{6}He)^{14}N at 15.5 MeV/nucleon. One of their DWBA calculations used a Gaussian potential of range 1.8 fm to model the interaction. This required a strength $G_{\sigma\tau} = 10.7$ MeV to reproduce their data. When converted by equivalencing the volume integrals, this corresponds to a single Yukawa of range 1.0 fm with a strength $V_{\sigma\tau} = 28$ MeV, which is close to our 14 MeV/nucleon result ($V_{\sigma\tau} = 23$ MeV) and also suggests that the one-step DWBA underpredicts the observed data at $E(^6\text{Li}) = 14$–16 MeV/nucleon.

Investigations with different tensor force strengths in the range 0.1 to 0.25 times the central force strength were carried out for ^{14}C(^{6}Li,^{6}He)^{14}N at 35 MeV/nucleon and are shown in Fig. 11. The optimum tensor to central force ratio at 35 MeV/nucleon was found to be 0.135. Tests with the ratio set to 0.1 and 0.2 showed that 0.135 was probably a reasonable choice at 25 and 14 MeV/nucleon energies also, and this value was used for all subsequent calculations. The effect of the inclusion of the tensor force was to increase the $L=2$ contribution to the cross section, thereby bringing the calculated angular distribution into better phase agreement with the data for angles larger than 3°. Calculations with little or no tensor force have a dominant contribution from $L=0$ and do not reproduce the data well. Although it is difficult to draw definitive conclusions in view of the neglect of the exchange contribution for the tensor interaction, a tensor force of strength about 1.7 MeV fm^{-2} best describes the 35 MeV/nucleon data. Given the uncertainties in the procedure, this agrees with the strength of up to 2.2 MeV fm^{-2} found[17] in an analysis of ^{26}Mg(^{6}Li,^{6}He)^{26}Al at 34 MeV and compares reasonably with the value of 3.2 MeV fm^{-2} which gave the best fit to the ^{25}Mg(^{6}Li,^{6}He) data in the same study.

TABLE III. Experimental and theoretical values for the Gamow-Teller strengths. The experimental values are from β-decay studies, while the theoretical values are from the overlap of the shell model wave functions used in the DWBA calculations. The ratio is used to renormalize the DWBA cross sections.

Transition	B(GT) expt.	B(GT) theory
^{12}C-^{12}N (0.0 MeV)	0.942	0.922
^{14}C-^{14}N (3.95 MeV)	2.8	4.04
^{26}Mg-^{26}Al (1.06 MeV)	0.64	0.87

B. ^{12}N(g.s.) and ^{26}Al(1.06 MeV)

Figure 12 shows DWBA predictions for the 1^+ ground state of ^{12}N and the 1.06-MeV state of ^{26}Al with a ^{6}Li bombarding energy of 35 MeV/nucleon. For ^{12}C(^{6}Li,^{6}He)^{12}N, a ^{6}Li+^{12}C optical potential from the compilation of Cook *et al.*[24] was used, while for ^{26}Mg(^{6}Li,^{6}He)^{26}Al, the global potential from Cook[39] was used. Again, several tensor to central force ratios were

TABLE IV. Values of direct (central) $V_{\sigma\tau}$ strengths required to fit the ^{14}C(^{6}Li,^{6}He)^{14}N(1^+, 3.95 MeV) data. The direct interaction had a Yukawa form with range 1.0 fm. The model assumed direct (D), knockon exchange (E), and tensor (T) interactions. Optical potential set $C1$ from Table II was used to generate the distorted waves.

E/A	Model	$V_{\sigma\tau}$ (MeV)
14	$D+E+T$	23
25	$D+E+T$	12
35	$D+E+T$	14.4[a]
35	$D+E$	14.5[a]
35	D	17[a]

[a]From a fit to data for $\theta_{c.m.} > 3°$.

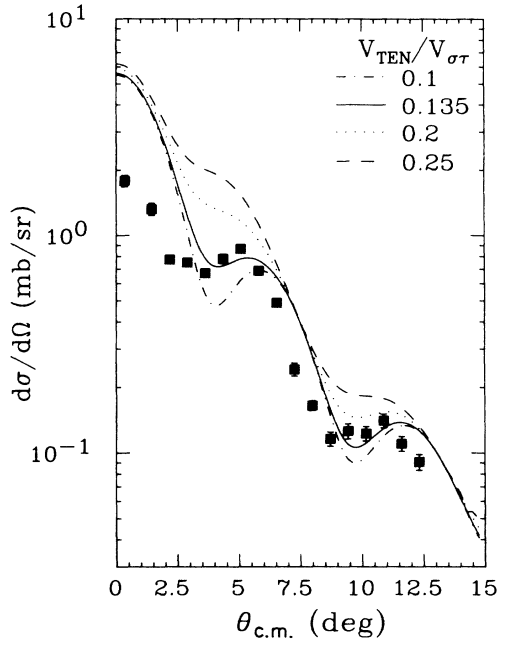

FIG. 11. Angular distribution and DWBA calculations for the reaction ^{14}C(^{6}Li,^{6}He)^{14}N (1^+, 3.95 MeV) at 35 MeV/nucleon with different tensor force strengths compared to the data. The same overall normalization factor is applied to all the calculations.

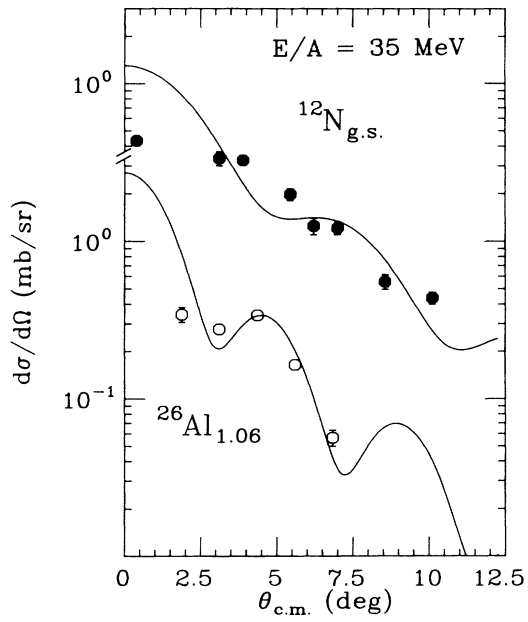

FIG. 12. Angular distributions for ^{12}C(^{6}Li,^{6}He)^{12}N$_{g.s.}$ and ^{26}Mg(^{6}Li,^{6}He)^{26}Al(1^+, 1.06 MeV) at $E(^6\text{Li})=35$ MeV/nucleon. The curves are microscopic DWBA calculations with a tensor force strength of 0.17 and 0.16 times the central ($V_{\sigma\tau}$) strength for ^{12}N and ^{26}Al, respectively. The calculations are normalized to the data (excluding $\theta_{c.m.}<2.5°$ for the ^{12}C target) to yield the empirical strengths of the interaction given in the text.

tried: The optimum fits to the data were found with a ratio of 0.17 for ^{12}N and 0.16 for ^{26}Al. The wave functions for the mass 12 system were again obtained from $1p$ shell-model calculations with the interaction of Millener;[40] for mass 26, the interaction of Wildenthal[44] and the full *sd* shell model space were used. Cross sections have been renormalized by the ratio of experimental to theoretical B(GT) values as indicated in Table III.

The very forward angle point for ^{12}C(^{6}Li,^{6}He)^{12}N is overpredicted by the DWBA, to an even greater extent than for ^{14}C(^{6}Li,^{6}He)^{14}N at 35 MeV/nucleon (Fig. 10). When the data for different targets are plotted as a function of qR, however, the 0° point for ^{12}N [at $qR/R(^{14}\text{C})=80$ MeV/c in Fig. 8] does not appear low, so the discrepancy is presumably a feature of the DWBA calculations.

The fit of the DWBA cross sections to the data (excluding the most forward angle point for ^{12}N) yields a central strength $V_{\sigma\tau}$ of 6 MeV for ^{12}N$_{g.s.}$ and 15 MeV for ^{26}Al (1.06 MeV). The value for ^{26}Al is in fair agreement with the accepted value from (p,n) and (p,p′) work.[43] The value for ^{12}N$_{g.s.}$ may still be within the range of uncertainties arising from the use of incorrect optical potentials, although the fit to the data is good (aside from the 0° point), and the same optical potential gave a reasonable value of $V_{\sigma\tau}$ for ^{14}N (3.95 MeV) at the same bombarding energy.

V. CROSS SECTIONS COMPARED WITH β-DECAY MATRIX ELEMENTS

The precision of DWBA analyses is often difficult to assess. However, DWBA calculations may be avoided by *calibrating* the (^{6}Li,^{6}He) probe with transitions for which the GT strength is known from β-decay studies. We therefore investigated how closely the observed cross sections at forward angles (where $L'=0$ transfers are strong) measure Gamow-Teller strength.

For (p,n) reactions at 120 MeV, the distortion-corrected 0° cross sections are observed[2] to be proportional to the squares of the respective matrix elements from β decay. Wharton and Debevec[13] have shown that even at $E(^6\text{Li})=34$ MeV, where multistep processes are known to give sizable contributions, there is still some correlation between (^{6}Li,^{6}He) $L'=0$ cross sections and the corresponding β-decay strength *within a given nucleus.* Some degree of correlation may be expected because, under certain conditions, the pickup-stripping amplitudes contain nuclear matrix elements similar to those which enter into the one-step spectroscopic amplitudes.[25] The data of Ref. 13 do show a marked nonmonotonic mass dependence across the *sd* shell, however.

Our results, which cover a mass range from 7 to 90, are shown in Fig. 13 as a plot of the observed cross section at $qR/R(^{14}\text{C})=100$ MeV/c vs B(GT) value, where q is the linear momentum transfer and $R/R(^{14}\text{C})$ is defined in the caption to Fig. 8. This value of $qR/R(^{14}\text{C})$ is close to the second maximum in the angular distributions. At $E/A=14$ MeV the overlap of equivalent qR values is too limited for comparison, but at 25 and 35 MeV/nucleon there is a high degree of proportionality for all final states

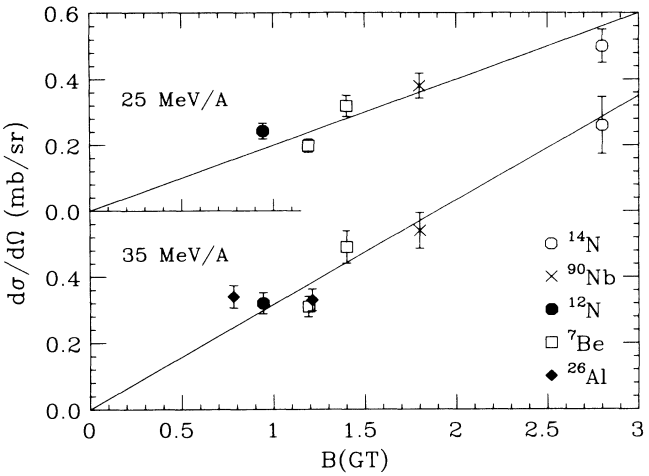

FIG. 13. Plot of experimental cross sections at $qR/R(^{14}C)=100$ MeV/c for various GT transitions induced by (^{6}Li,^{6}He) at 25 and 35 MeV/nucleon. The final states, with excitation energies in MeV, are ^{14}N (3.95), ^{90}Nb (2.3), ^{12}N (0.0), ^{7}Be (0.0 and 0.43), and ^{26}Al (1.06 and 1.85).

measured. The data for the ^{12}C and ^{90}Zr target do not extend to smaller values of $qR/R(^{14}C)$. However, the proportionality for the remaining data is as good at 60 MeV/c as at 100 MeV/c.

No correction for distortion effects has been applied to the points shown in Fig. 13, although such corrections are known to be important for the (p,n) $\langle$GT$\rangle$ correlations.[2,45] We have tried to estimate the distortion effects for (^{6}Li,^{6}He) but have not been able to obtain conclusive results. The procedure for the (p,n) case is to compare plane wave calculations with distorted-wave ones. For heavy ions, plane wave calculations do not give reasonable cross sections unless a lower cutoff radius is imposed on the integration to simulate the strong absorption. Unfortunately, the magnitudes of the cross sections are very sensitive to the choice of cutoff radius and, although some constraints may be made through the angular spacing of the diffraction oscillations, the resulting uncertainties are too great for a definitive result. In view of this, it is clear that further empirical calibration cases are necessary before the reaction may be applied to heavy targets.

The significance of Fig. 13 is that it allows one to determine GT strength [B(GT) values] for unknown transitions. We thus have a calibration of the (^{6}Li,^{6}He) reaction for use in the extension of measured spin transfer strength in nuclei.

VI. SUMMARY AND DISCUSSION

We have made an exploratory survey of the (^{6}Li,^{6}He) charge-exchange reaction at beam energies significantly higher than previously available. The reaction has been investigated on a wide range of targets ($A=7$–90), all of which have well-known GT transitions and have been studied previously with the (p,n) reaction.

The ^{14}C target presents several final states of particular interest in regard to the question of the reaction mechanism. Bombarding energy systematics are now available up to 35 MeV/nucleon. The observed ratio of the cross section for the IAS to that for the 1^+, 3.95 MeV state in ^{14}N shows a monotonic decrease with increasing $E(^6\text{Li})$, which indicates that the reaction mechanism becomes simpler at higher energies. This inference agrees with the predictions of von Oertzen[18] that the amplitude for processes involving nucleon transfer will decrease exponentially, whereas the cross sections for the quasielastic one-step process are expected[18,19] to remain essentially constant at intermediate energies. The measured cross section ratios for $(^{14}N_{g.s.})/(^{14}N_{3.95})$ and $(^{7}Be_{g.s.})/(^{7}Be_{0.43})$ add weight to the argument, but the details there are complicated by possible contributions from tensor or central $L=2$ amplitudes.

The microscopic one-step DWBA calculations we have performed have generally reproduced the data quite well, although discrepancies at very forward angles and some phase mismatch are present. A tensor force is required to give angular distributions with shapes which approximate the data. The strength of the tensor force we find is similar to that used in other (^{6}Li,^{6}He) work.[17] The central force strengths ($V_{\sigma\tau}$) required to fit the 35 and 25 MeV/nucleon data are generally in better agreement with Austin's estimate[43] of the NN interaction strength than found in lower energy (^{6}Li,^{6}He) work,[17,20] including the present results at 14 MeV/nucleon. As is usual in such DWBA studies, there is a degree of spread and uncertainty in the strengths of the forces extracted. This is partly because $V_{\sigma\tau}$ and V_{ten} were obtained from taking the best fit to the data despite the incompleteness of the calculation (e.g., the neglect of the exchange part of the tensor force) and the other approximations made. Additional uncertainties result from the choice of OM potentials and shell model wave functions.

We conclude that there is evidence for a "critical energy" in the (^{6}Li,^{6}He) reaction of about 25 MeV/nucleon, below which the contribution from multistep processes is increasingly noticeable. This value is consistent with the observation that the (p,n) reaction at energies above 25 MeV appears to be well described by a one-step mechanism.[21] For charge-exchange reactions with heavier ions, however, there still seems to be a significant contribution from sequential transfer at 20–35 MeV/nucleon: One-step predictions can account for only about 15% of the ^{12}C(^{12}C,^{12}N)^{12}B cross section at 35 MeV/nucleon (Ref. 19) and for only about 30% of that of the ^{28}Si(^{18}O,^{18}F)^{28}Al reaction at 20 MeV/nucleon.[46] The difference in the relative importance of the competing reaction processes between (^{6}Li,^{6}He), (^{12}C,^{12}N), and (^{18}O,^{18}F) is probably related in part to the difference in the β-decay strengths of the $A=6$, 12, and 18 systems: That for $^6\text{He}\rightarrow{}^6\text{Li}$ is 16 times larger than that for $^{12}\text{N}\rightarrow{}^{12}\text{C}$ and 4.2 times larger than that for $^{18}\text{F}\rightarrow{}^{18}\text{O}$, so the one-step process is correspondingly more favored in the (^{6}Li,^{6}He) reaction.

In the 35 MeV/nucleon spectra for ^{90}Zr(^{6}Li,^{6}He)^{90}Nb, the giant GT resonance which is so prominent in the ^{90}Zr(p,n)^{90}Nb data of Bainum *et al.*[31] is not pronounced and is estimated to account for about 40% of the yield be-

tween 6 and 11 MeV excitation. The remaining yield in this region presumably corresponds to higher-multipole spin-flip resonances, as suggested in the lower energy (15.5 MeV/nucleon) work by Dem'yanova *et al.*[33] For small scattering angles, the linear momentum transfer q for a given reaction scales approximately with energy *per nucleon* (see Fig. 14); thus at the substantially higher energies which will be available soon at heavy-ion facilities, q will be comparable to that in (p,n) studies with comparable isolation of $L'=0$ strength even for broad excitations. At intermediate bombarding energies, the GT strength for isolated states could be determined with very good resolution (perhaps as good as 50 keV) with high-performance spectrographs. Thus one has established a probe where the bombarding energy can be chosen to meet the most pressing needs for a particular experiment: resolution or L' isolation, always knowing that the spin transfer is $S=1$. In addition, the feature of strong absorption may be advantageous for cases where a node in the transition density occurs within the nucleus. An example is the spin-isovector-monopole transition: The cross section should be relatively larger for heavy-ion reactions since contributions from the exterior and interior will not cancel.

In order to avoid the uncertainties and ambiguities of a DWBA analysis, it is useful to calibrate the (^{6}Li,^{6}He) reaction by comparing the observed cross sections for GT transitions with the corresponding GT strength known from β decay [or, where necessary, from (p,n) studies]. This has been done at $E(^6\text{Li})=25$ and 35 MeV/nucleon and we find a striking linear relationship. With this result and the strong indications of the single-step nature of the reaction at these energies, it should be possible to measure accurate spin-transfer strengths with the (^{6}Li,^{6}He) reaction.

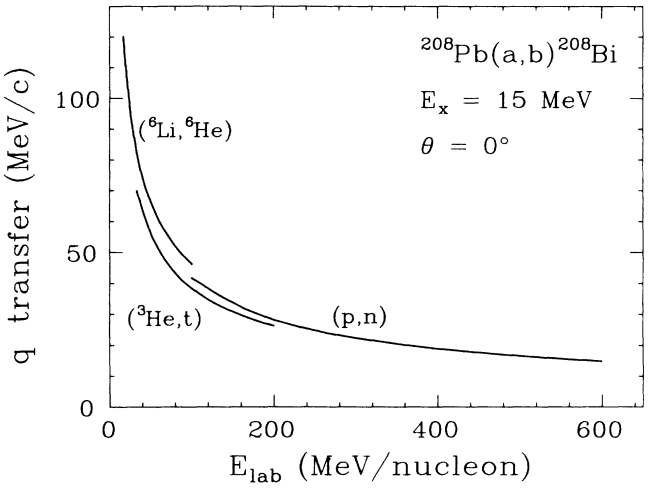

FIG. 14. The energy dependence of linear momentum transfer (q) for the charge exchange reaction on ^{208}Pb induced by p, ^{3}He, and ^{6}Li projectiles. The q transfer essentially scales with energy per nucleon apart from some small offsets due to the different Q values of the reactions.

ACKNOWLEDGMENTS

We would like to thank Dr. S. Gales for assistance in the early part of the experiments, Dr. G. Raisbeck for a communication, and Dr. G. F. Bertsch, Dr. B. A. Brown, and Dr. W. G. Love for helpful discussions. This work was supported in part by the National Science Foundation under Grants No. PHY83-12245 and PHY83-17437.

*Present address: Department of Physics, University of Groningen, 9718CM Groningen, The Netherlands.

†Present address: Physics Department, University of New Mexico, Albuquerque, NM 87131.

‡Present address: Schlumberger Well Services, Houston, TX 77210.

[1]C. D. Goodman, Nucl. Phys. **A374**, 241c (1982).

[2]C. D. Goodman, C. A. Goulding, M. B. Greenfield, J. Rapaport, D. E. Bainum, C. C. Foster, W. G. Love, and F. Petrovich, Phys. Rev. Lett. **44**, 1755 (1980).

[3]C. D. Goodman and S. D. Bloom, in *Spin Excitations in Nuclei,* edited by F. Petrovich *et al.* (Plenum, New York, 1984), p. 143; C. Glashausser, Comments Nucl. Part. Phys. **14**, 39 (1985), and references therein.

[4]C. Ellegaard *et al.*, Phys. Rev. Lett. **50**, 1745 (1983).

[5]W. C. Haxton, Comments Nucl. Part. Phys. **11**, 41 (1983).

[6]H. V. Klapdor, in *Progress in Particle and Nuclear Physics,* edited by D. Wilkinson (Pergamon, Oxford, 1983), Vol. 10, p. 131, and references therein.

[7]H. Orihara, S. Nishihara, K. Furukawa, T. Nakagawa, K. Maeda, K. Miura, and H. Ohnuma, Phys. Rev. Lett. **49**, 1318 (1982).

[8]A. B. Migdal, Rev. Mod. Phys. **50**, 107 (1978).

[9]W. R. Wharton and P. T. Debevec, Phys. Rev. Lett. **51B**, 451 (1974).

[10]C. Gaarde, T. Kammuri, and F. Osterfeld, Nucl. Phys. **A222**, 579 (1974).

[11]K.-I. Kubo, Nucl. Phys. **A246**, 246 (1975); F. Osterfeld and H. H. Wolter, Phys. Lett. **60B**, 253 (1976).

[12]H. H. Duhm, H. Hafner, R. Renfordt, M. Goldschmidt, O. Dragun, and K.-I. Kubo, Phys. Lett. **48B**, 1 (1974).

[13]W. R. Wharton and P. T. Debevec, Phys. Rev. C **11**, 1963 (1975).

[14]C. D. Goodman, W. R. Wharton, and D. C. Hensley, Phys. Lett. **64B**, 417 (1976).

[15]W. R. Wharton, C. D. Goodman, and D. C. Hensley, Phys. Rev. C **22**, 1138 (1980).

[16]A. Cunsolo, A. Foti, G. Imme, G. Pappalardo, G. Raciti, N. Saunier, and B. T. Kim, Nucl. Phys. **A355**, 261 (1981).

[17]G. Ciangaru, R. L. McGrath, and F. E. Cecil, Nucl. Phys. **A380**, 147 (1982); Phys. Lett. **61B**, 25 (1976).

[18]W. von Oertzen, in *Frontiers of Nuclear Dynamics,* edited by R. A. Broglia and C. H. Dasso (Plenum, New York, 1985), p. 241; W. von Oertzen, Phys. Lett. **151B**, 95 (1985).

[19]J. S. Winfield, N. Anantaraman, S. M. Austin, L. H. Harwood, J. van der Plicht, H.-L. Wu, and A. F. Zeller, Phys.

Rev. C **33**, 1333 (1986).
[20]D. V. Aleksandrov, Yu. A. Glukhov, A. S. Demyanova, A. A. Ogloblin, S. B. Sakuta, V. V. Suhkarevsky, S. V. Tolokonnikov, S. A. Fayans, F. A. Gareev, S. N. Ershov, I. N. Borzov, and J. Bang, Nucl. Phys. **A436**, 338 (1985).
[21]W. A. Sterrenburg, S. M. Austin, U. E. P. Berg, and R. P. DeVito, Phys. Lett. **91B**, 337 (1980).
[22]N. Anantaraman, J. S. Winfield, S. M. Austin, A. Galonsky, J. van der Plicht, C. C. Chang, G. Ciangaru, and S. Gales, Phys. Rev. Lett. **57**, 2375 (1986).
[23]B. M. Sherrill, Ph.D. thesis, Michigan State University, 1985 (to be published).
[24]J. Cook, H. J. Gils, H. Rebel, Z. Majka, and H. Klewe-Nebenius, Nucl. Phys. **A388**, 173 (1982).
[25]V. A. Madsen, in *The Two-Body Force in Nuclei,* edited by S. M. Austin and G. M. Crawley (Plenum, New York, 1972), p. 315.
[26]R. W. Kavanagh, Nucl. Phys. **A129**, 172 (1969).
[27]T. N. Taddeucci, R. R. Doering, A. Galonsky, and S. M. Austin, Phys. Rev. C **29**, 764 (1984).
[28]C. D. Goodman, in *Progress in Particle and Nuclear Physics,* edited by D. Wilkinson (Pergamon, Oxford, 1984), Vol. 11, p. 475.
[29]J. Atkinson and V. A. Madsen, Phys. Rev. C **1**, 1377 (1970).
[30]S. M. Austin, L. E. Young, R. R. Doering, R. DeVito, R. K. Bhowmik, and S. D. Schery, Phys. Rev. Lett. **44**, 972 (1980).
[31]D. E. Bainum, J. Rapaport, C. D. Goodman, D. J. Horen, C. C. Foster, M. B. Greenfield, and C. A. Goulding, Phys. Rev. Lett. **44**, 1751 (1980).
[32]R. R. Doering, A. Galonsky, D. M. Paterson, and G. F. Bertsch, Phys. Rev. Lett. **35**, 1691 (1975).
[33]A. S. Dem'yanova, S. A. Fayans, Yu. A. Glukhov, A. A. Ogloblin, S. B. Sakuta, S. N. Ershov, F. A. Gareev, and N. I. Pyatov, Nucl. Phys. **A444**, 519 (1985).
[34]P. D. Kunz, DWUCK4 (unpublished); extended version of J. R. Comfort (unpublished).
[35]W. G. Love, private communication.
[36]A. Etchegoyen, D. Sinclair, S. Liu, M. C. Etchegoyen, D. K. Scott, and D. L. Hendrie, Nucl. Phys. **A397**, 343 (1983).
[37]T. Tamura and K. S. Low, Comput. Phys. Commun. **8**, 349 (1974).
[38]W. G. Love and L. J. Parish, Nucl. Phys. **A157**, 625 (1970).
[39]J. Cook, Nucl. Phys. **A388**, 173 (1982).
[40]D. J. Millener, private communication.
[41]M. McMaster, G. Gunderson, A. Judd, S. Villaneuva, A. Nadasen, F. D. Becchetti, J. Janecke, P. Schwandt, J. S. Winfield, J. van der Plicht, R. E. Warner, and A. A. Cowley, Annual Report of the Michigan State University National Superconducting Cyclotron Laboratory, 1985 (unpublished), p. 93.
[42]G. Ciangaru, Nucl. Phys. **A398**, 371 (1983).
[43]S. M. Austin, in *The (p,n) Reaction and The Nucleon-Nucleon Force,* edited by C. D. Goodman *et al.* (Plenum, New York, 1980), p. 203.
[44]B. H. Wildenthal, in *Progress in Particle and Nuclear Physics,* edited by D. Wilkinson (Pergamon, Oxford, 1984), Vol. 11, p. 5.
[45]C. D. Goodman, in *The (p,n) Reaction and the Nucleon-Nucleon Force,* edited by C. D. Goodman *et al.* (Plenum, New York, 1980), p. 162.
[46]D. J. Horen, B. L. Burks, M. A. G. Fernandes, R. L. Auble, F. E. Bertrand, J. L. Blankenship, J. L. C. Ford, Jr., E. E. Gross, D. C. Hensley, R. O. Sayer, G. R. Satchler, D. Shapira, T. P. Sjoreen, and F. Petrovich, Phys. Lett. **181B**, 38 (1986).